

## Magnetoimpedance aftereffect in a soft magnetic amorphous wire

M. Knobel,\* M. L. Sartorelli, and J. P. Sinnecker†

*Instituto de Física “Gleb Wataghin,” Universidade Estadual de Campinas (UNICAMP), Caixa Postal 6165, 13.083-970 Campinas, São Paulo, Brazil*

(Received 12 November 1996)

A slow relaxation of the high-frequency impedance is observed in a  $\text{Co}_{68.25}\text{Fe}_{4.5}\text{Si}_{12.25}\text{B}_{15}$  amorphous wire after nucleation of a new domain pattern in a previously saturated sample. The observed impedance decay follows quasilogarithmic kinetics, and it is probably associated with the low-field ac magnetic permeability aftereffect of the circular domain walls. The impedance drop achieves relative amplitudes up to 1%, 16 s after the removal of the saturating external field. The effect is studied under typical magnetoimpedance experimental conditions, varying both the ac current amplitude and frequency. Although completely undesirable for many technical applications, the unique kinetic features of the impedance aftereffect may be explored to study circular magnetization processes under extreme domain-wall velocities. [S0163-1829(97)50410-3]

Although amorphous magnetic materials have been known for more than thirty years, their basic and applied interest has been constantly renewed, owing to the discovery of new and attractive properties. Recently, the observation of large field-induced changes in the high-frequency impedance of soft magnetic amorphous wires<sup>1-3</sup> and ribbons<sup>4,5</sup> opened enormous perspectives in the use of amorphous materials as cheap and sensitive magnetic-field sensors. When a high-frequency ( $f > 100$  kHz) and low-intensity ( $i < 15$  mA) electrical current flows through a soft magnetic material, its impedance suffers a strong variation if an external magnetic field is applied to the sample. This effect, known as giant magnetoimpedance (GMI), can be qualitatively understood in terms of field-induced changes in the magnetic penetration depth  $\delta_m$ :<sup>1,6</sup>

$$\delta_m = \sqrt{\frac{\rho}{\pi \mu f}}, \quad (1)$$

where  $\rho$  is the electrical resistivity,  $\mu$  is the transversal permeability (in the case of wires, it is the circular permeability), and  $f$  is the field (current) frequency. In a naive view, the application of a longitudinal dc magnetic field causes a strong variation in the transversal permeability, which is directly related to the imaginary component of the impedance (the reactance  $X$ ),<sup>3</sup> causing a strong change in the penetration depth, and therefore influencing also the real part of the impedance (the resistance  $R$ ).<sup>3</sup> Although rooted in classical electrodynamics, there are several aspects of GMI that remain to be understood, in particular, the role of induced anisotropies and the effect of different magnetization mechanisms in the observed phenomena.<sup>2-5</sup>

On the other hand, it is well known that after a sudden rearrangement of the magnetic domain structure in amorphous ferromagnetic materials, a relaxing behavior of the low-field permeability is observed at any temperature (up to  $T_c$ ), being characterized by quasilogarithmic relaxation kinetics.<sup>7,8</sup> This relaxation, also known as magnetic permeability aftereffect (MAE), or simply disaccommodation, has been explained in terms of directional ordering mechanisms of specific atoms, or atom pairs, interacting with the local

magnetization vector.<sup>7,8</sup> The time relaxation of the magnetic permeability is thought to be an intrinsic property of amorphous materials, basically related to structural defects (free volumes<sup>9</sup> or shear stresses<sup>10</sup>) inherent to the glassy structure. MAE is observed in amorphous ribbons of any composition, and it is characterized by a very broad distribution of time constants. A time decay of the axial permeability was reported also in amorphous wires, with similar relaxation intensities as found in amorphous ribbons.<sup>11</sup> Although the magnetic disaccommodation may be a drawback in certain applications of amorphous ferromagnets, this relaxation effect is generally useful to investigate the domain-wall behavior under different solicitations.<sup>12</sup>

In this paper we report that, under a typical GMI experiment, a nearly nonmagnetostrictive amorphous wire can display a long time relaxation of impedance. Because the impedance is strongly dependent on the magnetic permeability through the penetration depth [Eq. (1)], we associate the observed time decay of the impedance with the aftereffect of the *circular* permeability, which occurs after a sudden change of the domain structure. It is worth noticing that besides the technical importance of this relaxation effect, it opens the possibility of studying circular domain-wall dynamics, which is impossible to investigate using conventional methods.

In the present experiment we have used an as-cast  $\text{Co}_{68.25}\text{Fe}_{4.5}\text{Si}_{12.25}\text{B}_{15}$  amorphous wire (120  $\mu\text{m}$  diameter) produced by the in-rotating water quenching technique, whose room-temperature resistivity is nearly 1.3  $\mu\Omega\text{m}$ . The 8.0 cm long wire was positioned perpendicular to the earth magnetic field, in a Helmholtz coil system (maximum field  $H_{\text{max}} = 8$  kA/m). An ac current ( $i < 12$  mA,  $f < 1$  MHz) was generated by a EG&G 5302 lock-in amplifier, which also reads the in-phase and quadrature components of the voltage induced in the sample. The flowing current was constantly monitored in a standard resistor connected in series with the sample, and kept to a fixed value by a general purpose-interface bus (GPIB) controlled system. For the relaxation measurements, a fixed magnetic field of 2.6 kA/m is applied for 3 s, then it is switched off. The decay of the field occurs continuously, achieving zero in less than 5 ms. This time is

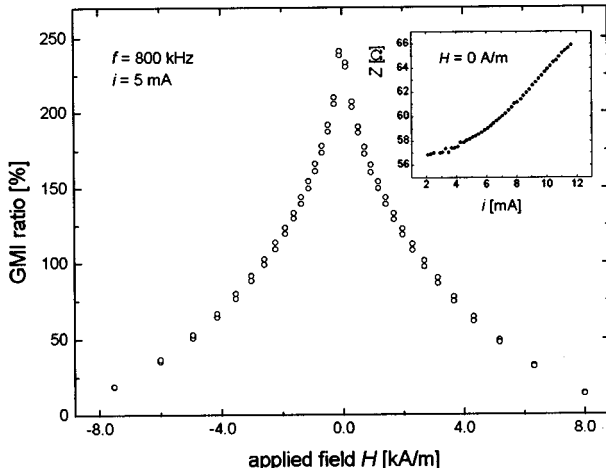


FIG. 1. Giant magnetoimpedance (GMI) ratio (defined in the text) as a function of the axial dc magnetic field  $H$ , for a driving current  $i=5$  mA ( $f=800$  kHz). The inset shows the total impedance  $Z$  as a function of the driving current amplitude  $i$ , for the same frequency and without the application of an external field.

defined as  $t=0$ , and both components of impedance are then monitored as a function of time (up to 16 s). The procedure is repeated 10 times for each value of the experimental parameters, to guarantee good statistics.

Figure 1 shows the field dependence of the giant magnetoimpedance ratio, defined as  $100 \times [Z(H) - Z(H_{\max})]/Z(H_{\max})$ , for a drive current amplitude  $i=5$  mA and frequency  $f=800$  kHz. The total magnetoimpedance ratios measured in this sample are similar to the ones reported in the literature,<sup>1,2,13</sup> achieving values up to 250% even without a complete saturation, as in the example shown in Fig. 1. It is important to clarify that although the voltage wave form measured in our sample at low applied fields displays a non-linear behavior, it is not so different from the driving current wave form (sinusoidal). In other words, we do not observe sharp spikes characteristic of a highly nonlinear relation between  $V(t)$  and  $I(t)$ ,<sup>14</sup> and therefore the linear impedance formalism can be employed to describe the observed effects.<sup>15</sup> The inset of Fig. 1 shows the behavior of the total impedance as a function of the driving current amplitude  $i$ , for a fixed frequency  $f=800$  kHz. The ac electrical current  $i$  gives rise to a circular magnetic field, which, in the case of a homogeneously distributed current is simply given by  $H_{\phi}(r) = ir/2\pi a^2$  ( $a$  being the wire radius). However, for the considered frequencies there is a significant skin effect, and therefore the circular field depends on the penetration depth, hindering a good estimation of the driving field in the vicinity of the wire's surface. Nevertheless, we do not observe a maximum in the impedance vs current curves (see inset of Fig. 1) and therefore we can state that the circular coercive force<sup>1</sup> is not achieved with 12 mA.

Figure 2 shows an example of the relaxation curves of both components of impedance obtained in our experiments, for  $i=0.1$  mA and  $f=500$  kHz. The times  $t_1=0.25$  s and  $t_2=16$  s are indicated in the figure, to evidence the time interval considered in our following analysis. Both curves shown in Fig. 2 are representative of all measured data, following a quasilogarithmic behavior in a large time interval. The relative changes in the impedance (from 0.25 s to 16 s)

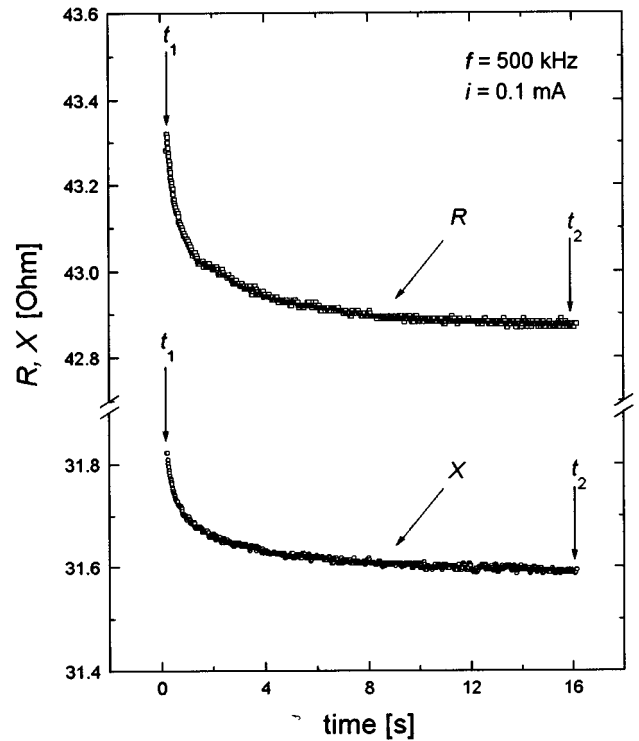


FIG. 2. Typical time dependence of both components of the complex impedance ( $Z=R+iX$ ) after the removal of a dc longitudinal magnetic field ( $H_{dc}=2.6$  kA/m) at  $t=0$  s. The fixed times  $t_1=0.25$  s and  $t_2=16$  s are used in the subsequent analysis.

can achieve values up to 1% (for high frequencies and low currents) for the studied amorphous wire. It is also interesting to note that the relaxation displays a rather slow kinetics, still approaching an equilibrium value even 16 seconds after the field removal. This fact prompted us to discard definitely an explanation of the data based merely on the expected relaxation in a circuit containing an inductive element. Considering a simple  $RL$  series circuit or an arrangement of  $RL$  circuits in series and parallel,<sup>16</sup> one obtains inductive time constants  $\tau$  never larger than tenths of  $\mu\text{s}$ , which are negligible in comparison with the observed impedance relaxation (e.g., in the case of Fig. 2, we consider  $R=9.2$   $\Omega$ ,  $L=11$   $\mu\text{H}$ , and therefore  $\tau=L/R=1.2$   $\mu\text{s}$ ). As pointed out before, the impedance is directly related to the circular magnetic permeability, whose component due to domain-wall movements is expected to decay after a sudden removal of the dc magnetic field. Furthermore, a considerable damping of the domain walls is expected from micro-eddy-currents,<sup>17</sup> which shall play an important role in the present working frequencies. Therefore, the observed impedance relaxation seems to be closely correlated with the damped circular domain-wall displacements, the origin of the damping being both by micro-eddy-currents and magnetic permeability aftereffect.

In order to verify the main cause of the observed relaxation, we have followed similar data analysis procedures to the ones done in the case of conventional disaccommodation measurements.<sup>8,12,18</sup> In the impulsive method, the decay amplitude is plotted as a function of the applied driving field (or induced magnetization) to detect a maximum, where the domain-wall displacement amplitude corresponds to approximately half of the domain-wall width.<sup>8,12</sup> Figure 3 shows the

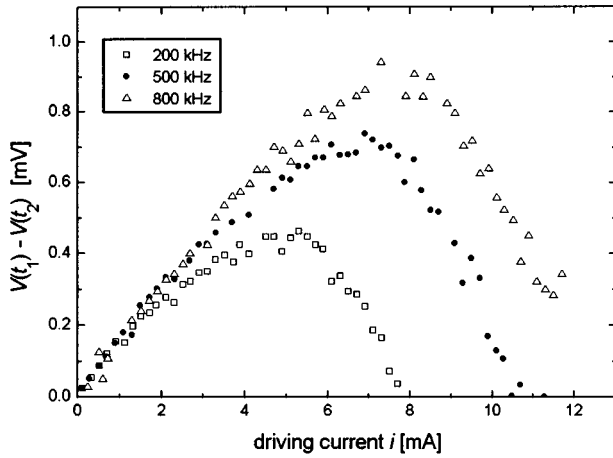


FIG. 3. Absolute time decay of the voltages directly measured in the amorphous wire,  $V(t_1) - V(t_2)$ , as functions of the applied current amplitude  $i$ , for three different current frequencies  $f$ .

absolute relaxation of the induced voltage in the wire  $V(t_1) - V(t_2)$  (analogous to  $\Delta B$  in conventional measurements), as a function of the applied electrical current  $i$  (corresponding to the driving field amplitude), for current frequencies of 200, 500, and 800 kHz. As shown in the inset of Fig. 1, we are working in the reversible region of the magnetization curve, in analogy with conventional aftereffect measurements.<sup>8,18</sup> Notice that all curves show a maximum, whose position displaces towards higher values with increasing frequencies. Considering that the domain-wall width remains the same for different frequencies, larger field amplitudes are necessary to overcome the damping due to eddy currents, and therefore the position of the maximum (corresponding to a particular area swapped by the circular domain walls) displaces towards larger current (field) values. There are, however, some interesting aspects that remain to be clarified. If we plot the same curve separating both in-phase and quadrature components of the induced voltage, the maxima appear in different positions, indicating that probably an extra contribution from the imaginary part of the magnetic permeability should be considered to explain the observed behavior. Furthermore, when one plots the impedance relaxation ( $\delta Z = Z(t_1) - Z(t_2) = [V(t_1) - V(t_2)]/i$  or  $\delta Z/Z = [Z(t_1) - Z(t_2)]/Z(t_2) = [V(t_1) - V(t_2)]/V(t_2)$ ) as functions of the applied current, the curves decrease continuously (for example, changing  $i$  from 0.1 to 8 mA,  $\delta Z/Z$  goes from 0.6 to 0.2% for  $f=200$  kHz and from 0.7 to 0.35% for  $f=800$  kHz), owing to the presence of  $i$  or  $V$  terms in the denominator. In such cases the increase in  $i$  and  $V$  is dominant in the absolute and relative impedance relaxations, respectively, which decay with increasing driving field amplitude.

Similar problems appear in the representation of the  $Z$  decay as a function of the driving field frequency. Figure 4 shows a frequency scan of the relaxation effect, from 100 to 900 kHz, for  $i=0.1$  mA and  $i=7.1$  mA. Notice that the absolute decay of resistance  $\delta R \equiv [R(t_1) - R(t_2)]$  [Fig. 4(a)] increases continuously with frequency, whereas the absolute decay of reactance  $\delta X \equiv [X(t_1) - X(t_2)]$  [Fig. 4(b)], seems to approach a saturation value, or even present a maximum for low  $i$  values. The increasing trend is unexpected, once the damping of domain walls is presumed to increase, and the

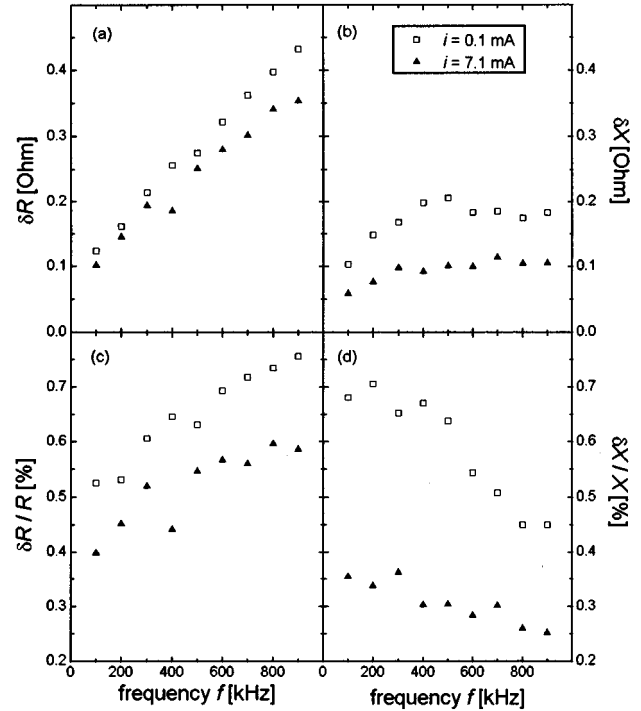


FIG. 4. Frequency dependence of absolute and relative relaxation amplitudes of both components of the impedance: (a) the absolute resistance  $R$  decay ( $\delta R$ ); (b) the absolute reactance  $X$  decay ( $\delta X$ ); (c) the relative  $R$  decay ( $\delta R/R$ ); and (d) the relative  $X$  decay ( $\delta X/X$ ). See details in text.

magnetic moments rotations are expected to prevail with increasing driving field frequencies. In fact, the increasing tendency could be due to an amplification effect produced by the crescent frequencies, which continuously reduce the penetration depth (proportional to  $1/\sqrt{f}$ ), even if the permeability drop remains constant or slightly decreases. While in the resistive component of the impedance the increase with frequency is dominant [see Fig. 4(a)], the reactive component trend [Fig. 4(b)] reflects the diminution of the relaxation effect at high frequencies ( $X \propto \mu f$ ).<sup>3</sup> The direct frequency amplification is avoided in the relative impedance decay plots [ $\delta R/R$  and  $\delta X/X$  vs  $f$ , in Figs. 4(c) and 4(d), respectively], owing to the presence of the impedance terms in the denominator. However, the real behavior of the relaxation effect is masked again, because both  $R$  and  $X$  increase with frequency. It is worth noticing that while the relative reactance decay follows the expected behavior [see Fig. 4(d)], the relative relaxation amplitude of the resistive component increases with frequency [Fig. 4(c)], indicating again that an extra contribution to the resistive component of the impedance must be considered to explain the observed behavior. As the two impedance components have opposite tendencies, the total impedance variation is almost independent of frequency, showing a slight increase for certain applied currents [e.g., going from 0.4% ( $f=100$  kHz) to 0.45% ( $f=900$  kHz) for  $i=7.1$  mA].

In prospective applications of amorphous wires as sensing elements, slow relaxation kinetics is completely undesirable. The data shown in this work indicate that it is very important to choose properly the frequency and amplitude of the electrical current, in order to minimize the impedance decay in

possible applications of the GMI effect. In the studied sample, the relative ratio of the relaxation effect is reduced for higher current amplitudes and lower current frequencies. Considering the frequencies shown in Fig. 3,  $\delta Z/Z$  is lower than 0.5% for  $i > 3.5$  mA,  $i > 4$  mA, and  $i > 6$  mA, for  $f = 200$  kHz, 500 kHz, and 800 kHz, respectively. Notice, however, that these relaxation ratios can achieve much larger values depending on the magnetostriction constant  $\lambda_s$  of the sample, because the disaccommodation amplitude is directly proportional to the square of  $\lambda_s$ .<sup>12</sup> As no significant contribution to MAE is expected from coherent magnetization rotation processes, in basic investigations the impedance aftereffect can be a useful tool to study, in particular, the fraction of the circular magnetization process which is actually carried out through 180° domain-wall motion.

In conclusion, we have observed a slow kinetics relax-

ation effect in the impedance of a soft magnetic amorphous wire, under common operative conditions. The total relaxation effect can achieve values up to 1% of the wire impedance, 16 seconds after a rapid external field removal. Although further studies are necessary to understand completely the impedance aftereffect, it is certainly an important factor to be taken into account in possible applications of the GMI. Furthermore, the impedance relaxation can be properly explored in the near future to deeper studies on high-frequency circular domain-wall displacements.

We acknowledge Dr. H. Chiriac from the Institute of Technical Physics, Iasi, Romania, for providing the amorphous wire and for helpful discussions during his visit to Campinas. This work was partially supported by FAPESP and CNPq (Brazilian agencies).

\*Electronic address: knobel@ifi.unicamp.br

†Present address: Instituto de Magnetismo Aplicado, Ap. Correos 155, Las Rozas, Madrid, Spain.

<sup>1</sup>R. S. Beach and A. E. Berkowitz, *Appl. Phys. Lett.* **64**, 3652 (1994).

<sup>2</sup>L. Panina and K. Mohri, *Appl. Phys. Lett.* **65**, 1189 (1994).

<sup>3</sup>M. Knobel, M. L. Sánchez, C. Gómez-Polo, P. Marín, M. Vázquez, and S. Hernando, *J. Appl. Phys.* **79**, 11 646 (1996).

<sup>4</sup>F. L. A. Machado, C. S. Martins, and S. M. Rezende, *Phys. Rev. B* **51**, 3926 (1995).

<sup>5</sup>R. Sommer and C. L. Chien, *Appl. Phys. Lett.* **67**, 857 (1995).

<sup>6</sup>L. D. Landau and E. M. Lifshitz, *Electrodynamics of Continuous Media* (Pergamon, Oxford, 1975), p. 195.

<sup>7</sup>H. Kronmüller and N. Moser, in *Amorphous Metallic Alloys*, edited by F. E. Luborsky (Butterworths, London/Washington, 1983), p. 341.

<sup>8</sup>P. Allia and F. Vinai, *Philos. Mag. B* **61**, 763 (1990).

<sup>9</sup>H. Kronmüller, *Philos. Mag. B* **48**, 127 (1983).

<sup>10</sup>P. Allia and F. Vinai, *Phys. Rev. B* **33**, 422 (1986).

<sup>11</sup>S. P. Cruz Filho, M. Knobel, J. P. Sinnecker, R. Sato Turtelli, and M. Vázquez, *J. Magn. Magn. Mater.* **104-107**, 105 (1992).

<sup>12</sup>P. Allia, C. Beatrice, and F. Vinai, in *Magnetoelastic Effects and Applications*, edited by L. Lanotte (Elsevier, Amsterdam, 1993), p. 47.

<sup>13</sup>M. Knobel, M. L. Sánchez, J. Velázquez, and M. Vázquez, *J. Phys., Condens. Matter.* **7**, L-115 (1995).

<sup>14</sup>R. S. Beach, N. Smith, C. L. Platt, F. Jeffers, and A. E. Berkowitz, *Appl. Phys. Lett.* **68**, 2753 (1996).

<sup>15</sup>L. V. Panina, K. Mohri, T. Uchiyama, and M. Noda, *IEEE Trans. Magn.* **31**, 1249 (1995).

<sup>16</sup>R. Valenzuela, M. Knobel, M. Vázquez, and A. Hernando, *J. Appl. Phys.* **78**, 5189 (1995); *J. Phys. D* **28**, 2404 (1995).

<sup>17</sup>B. D. Cullity, *Introduction to Magnetic Materials* (Addison-Wesley, Reading, Massachusetts, 1972), p. 464.

<sup>18</sup>J. P. Sinnecker, R. Sato Turtelli, M. Knobel, and J. F. Saenger, *IEEE Trans. Magn.* **30**, 1067 (1994).